Development of a Intelligent Welding Carriage for Automation of Curved Block

H.B. Choi*, J.H. Moon**, W.R. Jun*, and S.H. Kim

*Automation Research Part, SAMSUNG HEAVY INDUSTRIES, Seoul 123-456, Korea
(Tel: +82-55-630-6281; Fax: +82-55-630-5562; Email:{hb7.choi,biogreen.jun,sh3.kim}@samsung.com)
**Welding Research Part, SAMSUNG HEAVY INDUSTRIES, Seoul 123-456, Korea
(Tel: +82-55-630-6226; Fax: +82-55-630-5562; Email:jonghyun.moon@samsung.com)

Abstract: This paper presents a novel Intelligent-Welding-Carriage (IWC) for automation of curved block in shipbuilding. The curved block is usually used in both front and back side of the ship. In curved block root gap is big, 1∼7 [mm] and inclination, 0∼30 [deg]. Since available conventional carriage type is limited to use below root gap of 3 [mm], only manual welding is employed in curved block. To adopt an IWC in curved block, it requires control of the welding conditions, i.e., voltage, current and travel speed, with respect to root gap and inclination to achieve good welding quality. In this paper, an IWC is developed for automization of welding operation to accommodate gap and inclination. Kinematics model and dynamics using Lagrangian formulation of the manipulator is introduced. IWC utilizes a database to perform accurate welding. The database is programmed based on numerous experimental test results with respect to gap, inclination, material, travel speed, weaving condition, voltage, and current. Finally, experimental result using PID control is addressed for verify the trajectory tracking accuracy of end-effector.

Keywords: Welding, Carriage, Curved-Block, Shipbuilding, Automization

1. Introduction

Recently, due to the shortage and aging of experienced manpower, the development of robot-controlled automatic arc welding been encouraged. Despite the increasing importance of automation, i.e., welding, blasting, painting and coating activities as well as the increasing difficulties in finding workers, no substantial steps have been taken towards the welding automation. Many efforts for automation in shipbuilding have been applied almost exclusively in subassembly line [1][2][3][4].

In the shipbuilding, welding automation in a factory developed drastically. On the other hand, welding in a curved block still depends on by manual operation mainly. Especially, welding of a curved block is done by a skilled welder manually, because it is difficult to weld it automatically in the curved block as shown in Figure 1.

It is important to reduce production time, and costs by raising productivity in industrial work. Moreover, reduction of welding construction costs is strongly required and therefore, to cope with this demand in the field of arc welding, there has been a significant trend of increasing welding efficiency, improving at the same time the quality of welds. Automated welding system always aims at higher efficiency production, regarding the welding processes as core axes, then robot programming systems, seam tracking and adaptive control, welding robots and automated machines, are comprised as the basic systems.

(a) Gas Carrier

(b) Curved Block

Fig. 1. LNGC and Curved Block

Y. Sugitani developed lattice welding robot [5]. This robots consists of a high speed rotating arc welding torch, 2-axis slide blocks and a self-driven carriage. A. Aoki suggested a multi-purpose welding robot system [6]. It is provided with portable and modularized system component equipment. D.Y. Lee, *et. al.* proposed a new system for automatic transfer of the LNGC (Liquefied Natural Gas Carrier) membrane plasma welding-machine [7].

In this paper, for the purpose of high efficiency welding of the curved block, we developed an Intelligent Welding Carriage System. It is the sensor-aided and self-driven welding robot and its purpose is fully automatic welding of the curved block.

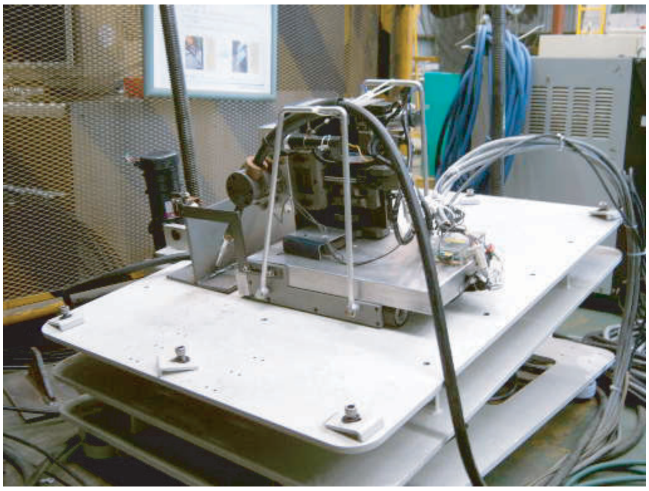

Fig. 2. Intelligent Welding Carriage System

2. System Configuration

In this study, we consider an IWC system that consists of a four-linked manipulator mounted at the center point of a four-wheeled mobile-platform. The basic concept of IWC is described Figure 2.

2.1. Motors

The IWC employs DC type motors embodying encoders. The maximum torque, rated speed and assigned power rating are 26.3 [mNm], 11000 [rpm] and 20 [W], respectively.

2.2. Motion Controller

For the control of IWC motion controller developed by SHI Mechatronics Research Team is adopted [7]. Using this controller 8 axes can be controlled. Controller is consist of controllers, power supplies for sensor and motors.

PID control is just used for IWC. The controller decodes the feedback signal of the encoder with the sampling of regular interval, based on the programmed position and speed of the host computer.

2.3. Sensors

Laser Vision Sensor(LVS) is used for seam tracking and checking gap. Limit sensors are applied to each axis to check the axes end. Especially, x-axis, driving direction, the proximity sensor is used. Moreover, inclinometer CXTA02, Crossbow, is employed for sensing the tilting angle of IWC. The tilting sensor have dual axis and angular range is $\pm$ 75 [deg].

2.4. Motion Table

For the welding test as in curved block, Motion Table is developed. Using this table, welding test can be achieved $\pm$35 [deg]. And magnetic is set on the bottom side to prevent the falling of IWC.

3. Kinematics of ICS

In this section, the inverse kinematics of ICS is considered. This chapter will be devoted to the kinematics of the IWC which means studying geometrically the motion of the IWC links. Kinematics deals with the aspects of motion without regard to the forces and torques that cause it or result from the motion [9]. Inverse kinematics is to find all possible sets of actuated joint variables and their corresponding time derivatives which will bring the travelling plate to the set of desired positions and orientations, On the other hand, forward kinematics is to find all possible sets of travelling plate positions and orientations.

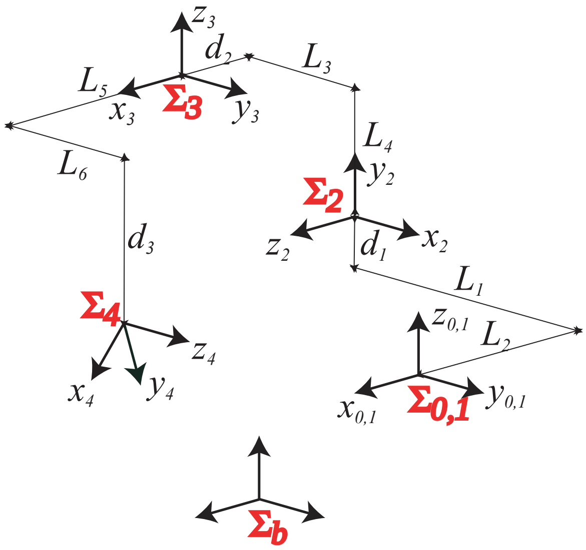

Fig. 3. Design parameters

Table 1. Link parameters of the IWC

i	α_{i-1} [deg]	a_{i-1} [mm]	d_i [mm]	a_i [deg]
1	0	0	0	θ_1
2	90	L_1	d_2	0
3	-90	L_3	d_3	-90
4	-90	L_5	L_6	θ_4

Typically, as the number of kinematic chains increases, the forward kinematics becomes more difficult. It is well known that in the case of a 6-DOF conventional serial robot the forward kinematics is relatively simple, while the inverse kinematics is difficult. To express the positions and orientations of the IWC, a assignment of a coordinate frame will be explained.

3.1. Inverse Kinematics

The prototype of the Intelligent welding system is illustrated in Figure 3. The link parameters corresponding to this placement of link frames are shown in Table 1. The link transformations can be defined as follows: Finally, we obtain the product of all four link transforms as follows:

$$
\begin{aligned}
{}^0\boldsymbol{T}_4 &= {}^0\boldsymbol{T}_1{}^1\boldsymbol{T}_2{}^2\boldsymbol{T}_3{}^3\boldsymbol{T}_4 \\
&= \begin{bmatrix} C\theta_4 S\theta_1 & -S\theta_1 S\theta_4 & -C\theta_1 & p_x \\ -C\theta_1 C\theta_4 & C\theta_1 S\theta_4 & -S\theta_1 & p_y \\ -S\theta_4 & -C\theta_4 & 0 & p_z \\ 0 & 0 & 0 & 1 \end{bmatrix}
\end{aligned} \tag{1}
$$

where,

$$
\begin{aligned}
p_x &= C\theta_1 L_1 + S\theta_1 L_2 + C\theta_1 L_3 + S\theta_2 L_5 - C\theta_1 L6 \\
p_y &= -S\theta_1 L_1 - C\theta_1 L_2 - S\theta_1 L_3 - C\theta_2 L_5 + S\theta_1 L6 \\
p_z &= L_4
\end{aligned}
$$

with, L_1, L_3, L_5, L_6, and d_3 are 100 [mm], 50 [mm], 120 [mm], 50 [mm], and 50 [mm], respectively.

4. Dynamics of ICS

We assume that the mobile-platform and the manipulator move at low speed because the welding velocity is just about 7.5 [mm/s] hence we ignore the inertia and the slipping between the wheels and the floor, so we only consider the kinematic representation for the mobile manipulator.

4.1. Notations

The terminologies which are used in this paper are represented as follows:

r	radius of the wheel
θ_i	angle of ith revolute joint
$\dot{\theta}_i$	angular velocity of ith revolute joint
d_i	distance of ith prismatic joint
$\dot{d}_i$	velocity of ith prismatic joint
m_b	the mass of the driving wheel
m_w	the mass of the platform without the driving wheels
m_i	the mass of the ith link of the manipulator
I_p	the moment of inertia of the platform without driving wheels
I_w	the moment of inertia of the driving wheel about the wheel axis
$I_{i_{xx}}$	the moment of inertia of the ith link about the X-axis
$I_{i_{yy}}$	the moment of inertia of the ith link about the Y-axis
$I_{i_{zz}}$	the moment of inertia of the ith link about the Z-axis

4.2. Lagrangian Formulation

In contrast to kinematics which deals with the geometry and time-dependent aspects of motion without considering the forces causing motion, dynamics based on kinematics includes the effect of the inertia forces. Dynamics is one of a very complicated subject. Typically, dynamics is described in terms of the time rate of change of a given travelling plate's trajectory in relation to the joint torque exerted by the actuators. The actuating torque would depend not only on a given trajectory but also on the mass properties of the links, and external forces. There are two types of dynamical analysis problems namely forward dynamics and inverse dynamics.

Dynamics are useful for computer simulation, the design of suitable control equations, and the evaluation of the kinematic design. For the real time control, the computational efficiency of inverse dynamics is one of the important issues. As an alternative methods for dynamics analysis, such as the Newton-Euler method, the Lagrangian methods, and the principle of virtual work can be applied. In this section, the Dynamics of ICS is addressed using Lagrangian formulation. The Lagrange equation of motion for the mobile manipulator is given as

$$
\boldsymbol{\tau} = \frac{d}{dt}\frac{\partial L}{\partial \dot{\boldsymbol{q}}} - \frac{\partial L}{\partial \boldsymbol{q}} \tag{2}
$$

where

$$
\begin{aligned}
\boldsymbol{q} &= [\theta_1 \;\; \theta_2 \;\; \theta_3 \;\; \theta_4 \;\; \theta_w]^{\mathrm{T}} \\
\boldsymbol{\tau} &= [\tau_1 \;\; \tau_2 \;\; \tau_3 \;\; \tau_4 \;\; \tau_w]^{\mathrm{T}}
\end{aligned}
$$

Here, θ_1, θ_2, θ_3 and θ_4 are the angular displacement of the joint and θ_1, θ_2, θ_3 and θ_4 are the torques action on the joint and wheel axis generated by actuators. Equation 3 can be expressed as follows:

$$
\boldsymbol{\tau} = \frac{d}{dt}\frac{\partial k}{\partial \dot{\boldsymbol{q}}} - \frac{\partial k}{\partial \boldsymbol{q}} + \frac{\partial u}{\partial \boldsymbol{q}}, \tag{3}
$$

where, k is the kinetic energy of the ith link and u is the potential energy of the ith link.

In this paper since the velocity of the mobile platform is as slow as the inertia can be ignored, we just consider that the Lagrangian is reduced to the kinetic energy K.

$$
L = k_p + k_m - u_p \tag{4}
$$

where k_p, k_m, and u_m are the kinetic energies of the mobile platform and the manipulator, and potential energy of manipulator, respectively. These can be expressed as follows:

$$
\begin{aligned}
k_p &= \frac{1}{2}(m_b + m_w)({}^b\dot{x}_0^2 + {}^b\dot{y}_0^2) + I_w {}^b\omega_w^2 \\
k_m &= k_1 + k_2 + k_3 + k_4 \\
&= \frac{1}{4}\Big[A\dot{d}_2^2 + B\dot{L}_4^2 + C\dot{d}_2\dot{\theta}_1 + A\dot{d}_2^2\dot{\theta}_1^2 + Dd_2\dot{\theta}_1^2 \\
&\quad + (E + FC\theta_4 + GC2\theta_4)\dot{\theta}_1^2 - HC\theta_4\dot{L}_4\dot{\theta}_4 \\
&\quad + JS\theta_4\dot{\theta}_1\dot{\theta}_4 + 2G\dot{\theta}_4^2\Big] + \frac{1}{2}(I_{1_{zz}} + I_{2_{yy}} + I_{zz})\dot{\theta}_1^2 \\
&\quad + \frac{1}{2}(I_{4_{xx}}\mathrm{S}\theta_4^2 + I_{4_{yy}}\mathrm{C}\theta_4^2 + I_{4_{zz}}\dot{\theta}_4^2) \\
u_p &= -\, m_3 g(L_4 + L_{4_{max}}) - m_4 g L_7(\mathrm{S}\theta_4 + 1)
\end{aligned} \tag{5}
$$

where,

$$
\begin{aligned}
A &= 2m_2 \\
B &= 2(m_2 + m_3 + m_4) \\
C &= 4(-L_1 + L_3)m_2 \\
D &= 4L_2 m_2 \\
E &= (2L_1^2 + 2L_2^2)m_1 + (2L_1^2 + 2L_2^2 - 4L_1L3 + 2L_3^2)m2 \\
&\quad + (2L_1^2 + 2L_2^2 + 4L_1L_3 + 2L_3^2 + 4L_2L_5 + 2L_5^2 \\
&\quad - 4L_1L_6 - 4L_3L_6 + 2L_6^2)m_3 + (2L_1^2 + 2L_2^2 + 4L_1L_3 \\
&\quad + 2L_3^2 + 4L_2L_5 + 2L_5^2 - 4L_1L_6 - 4L_3L_6 + 2L_6^2 + L_7^2)m_4 \\
F &= 4(L_2 + L_5)L_7 m_4 \\
G &= L_7^2 m_4 \\
H &= 4L_7 m_4 \\
J &= 4(L_1 + L_3 - L_6)L_7 m_4
\end{aligned}
$$

Dynamic equation of motion for the mobile manipulator is given in the vector form as follows:

$$
\boldsymbol{\tau} = \boldsymbol{M}(\boldsymbol{q})\ddot{\boldsymbol{q}} + \boldsymbol{N}(\boldsymbol{q}, \dot{\boldsymbol{q}}) + \boldsymbol{G}(\boldsymbol{q}) \tag{6}
$$

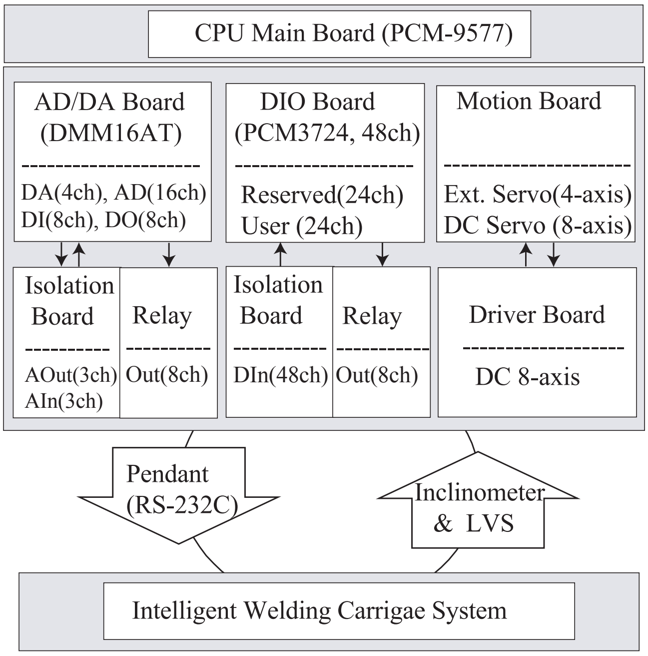

Fig. 4. System Configuration

where, $\boldsymbol{M}(\boldsymbol{q})$, $\boldsymbol{N}(\boldsymbol{q})$, and $\boldsymbol{G}(\boldsymbol{q})$ are the 5×5 inertia matrix which is the function of the angular displacements for the joints and wheels, the 5×1 torque vector due to coriolis and centrifugal terms, and is an 5×1 vector of gravity terms.

5. Experimental Result

In this section, the dynamics of ICS is considered. The velocity of the end-effector must keep up the welding velocity in the whole welding process.

For real-time controll RT-LINUX is used for IWC. RT-LINUX was developed by Finite State Machine, Inc. It works by patching the standard Linux kernel with the real-time plug-in. The real-time plug-in is in itself a small predictable operating system. It have its own scheduler and interrupt

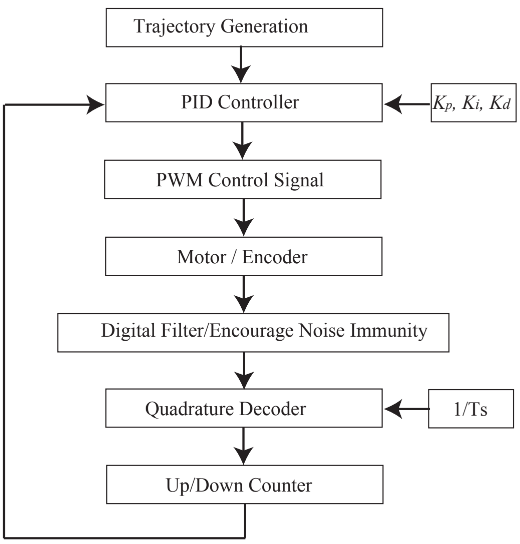

Fig. 5. Block diagram of PD control

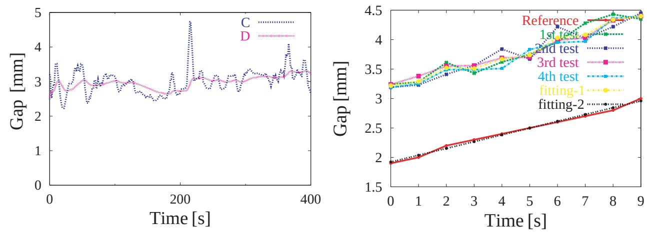

(a) Stiffener (b) Angle

Fig. 6. Comparision of gap data

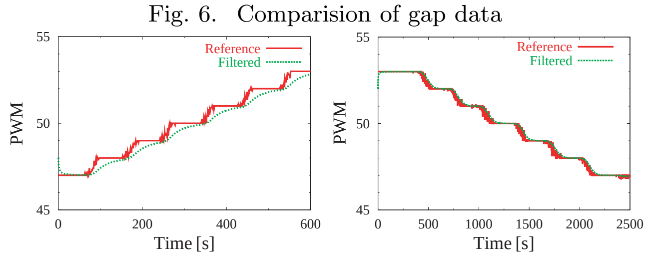

(a) X axis (b) Y axis

Fig. 7. Comparision of x-y inclinations

(a) Start point (b) End point

Fig. 8. Rotating of the end effector

handlers. To compare the performance characteristic such as trajectory and control, the PID control methods are applied as shown Figure 5. The data from the LVS are not suitable to use directly. Therefore, in this system we adopted the Kalman filter as shown Figure 6 (a). In case of Angle the end is rounded. Since it caused the gap error, less productivity with poor quality of weld and high repair rate. To reduce this problem, the gap resolution test is achieved shown Figure 6 (b).

The torch angle should be changed as the slop is increasing. However, as shown Figure 7 (a), (b) the inclination data is not linear. Therefore the Kalman filter is also adopted to minimize the difference of inclination data.

To verify trajectory tracking accuracy of the torch end, the experimentation accomplished as shown Figure 8 (a), (b). The experimental results are shown in Figure 9 (a) (d). Total time, Sampling time, starting point, and end point are 70 [s], 20 [ms], (-5,0,0) and (25,0,0), respectively. In the experiment, the control gains, K_p and K_d were set to 500 [s^{-1}] and 2.5, respectively. For this experimentation the total 5-DOF is reduced to 3-DOF. Therefore the inverse kinematics of manipulator could be solved as 2-DOF problem (see Appendix). In each figure, (a), (b), (c), and (d) represent the desired traveling plate trajectory with the current traveling

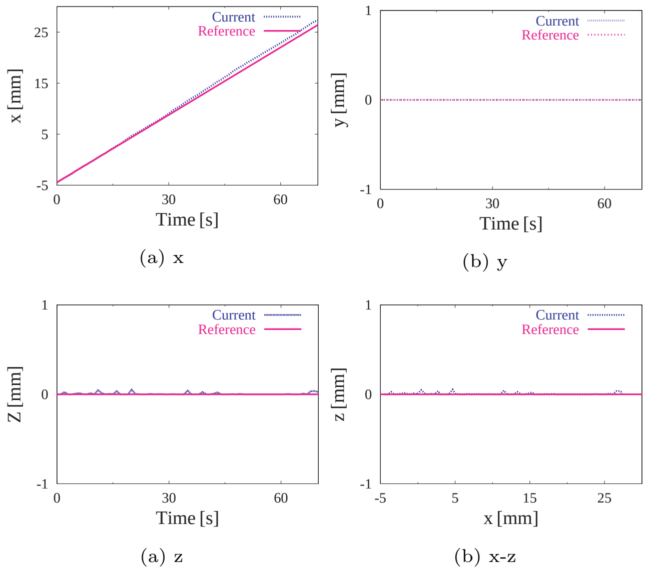

Fig. 9. Comparision of x-y inclinations

plate trajectory of x, y, z, and x−z, respectively.
In the result of PID control, there is a considerable delay in position (Figure 9) (a). The trajectory traking error is becoming greater at the end point than start point. This error could be reduced by adopting PD + feed forward, etc.

6. Conclusion

In this paper, we presented a novel Intelligent-Welding-Carriage (IWC) for automation of curved block. The IWC is developed for automization of welding operation to accommodate gap and inclination. Kinematic model of the manipulator is introduced. Kinematics and Dynamics of IWC are addressed in order to adopt trajectory tracking control.
IWC can utilize a database to perform accurate welding. The database is programmed based on numerous experimental test results with respect to gap, inclination, material, travel speed, weaving condition, voltage, and current. This experimental results demonstrated that the IWC is promising as a good welding mechanism.

Appendix

The inverse kinematics of IWC as 2-DOF can be calculated as follows:

$$[{}^0\boldsymbol{T}_1]^{-1}\,{}^0\boldsymbol{T}_3 = {}^1\boldsymbol{T}_2\,{}^2\boldsymbol{T}_3. \tag{7}$$

Equating the (1,4) elements from both sides of Equation 7, we have

$$C\theta_1 p_x + S\theta_1 p_y = l_1 + l_2 \tag{8}$$

To solve an equation of this form, we make the trigonometric substitutions

$$p_x = \rho S\phi, \qquad p_y = \rho C\phi \tag{9}$$

where

$$\rho = \sqrt{p_x^2 + p_y^2}, \qquad \phi = \mathrm{Atan2}(p_x, p_y)$$

Substitutiong Equation 9 into Equation 8, we obtain

$$S\theta_1 C\phi + C\theta_1 S\phi = \frac{l_1 + l_2}{\rho} \tag{10}$$

Using the difference of angles formula:

$$S(\theta_1 + \phi) = \frac{l_1 + l_2}{\rho} \tag{11}$$

Hence

$$C(\theta_1 + \phi) = \pm\sqrt{1 - \frac{(l_1 + l_2)^2}{\rho^2}} \tag{12}$$

and so

$$\theta_1 + \phi = \mathrm{Atan2}\left(\frac{l_1 + l_2}{\rho}, \pm\sqrt{1 - \frac{(l_1 + l_2)^2}{\rho^2}}\right) \tag{13}$$

Finally, the solution for θ_1 may be written:

$$\theta_1 = \mathrm{Atan2}\left(\frac{l_1 + l_2}{\rho}, \pm\sqrt{1 - \frac{(l_1 + l_2)^2}{\rho^2}}\right) - \mathrm{Atan2}(p_x, p_y) \tag{14}$$

Now tha θ_1 is known, the left-hand side of Equation 7 is known. If we equate the (1,4) elements from both sides of Equation 7, we obtain

$$-S\theta_1 p_x + C\theta_1 p_y = -C\theta_2 l_3 - d \tag{15}$$

From Equation 15,

$$d = S\theta_1 p_x - C\theta_1 p_y - C\theta_2 l_3 \tag{16}$$

References

[1] T. Miyazaki, Y. Nakashima and et. al, “NC Painting Robot for Shipbuilding”, *Proc. ICCAS’99*, 1999

[2] Kim J.H., Do G.S. and Yoon J.W., “Information Management for Automation of Sub-assembly Welding Line in Shipbuilding”, *2nd Asian Control Conference*, 1997

[3] T.T. Phan, T.L. Chung, M.D. Ngo, H.K. Kim, and S.B. Kim, “Decentralized Control Design for Welding Mobile Manipulator”, *Journal of Mechanical Science and Technology*, vol. 19, no. 3, pp. 756–767, 2005

[4] Yoo, W.S., Kim, J.D. and Na, S.J., “A Study on a Mobile-Platform Manipulator Welding System for Horizontal Fillet Joints”, *Trans, Mechatronics*, vol. 11, pp. 853–868, 2001

[5] Y. Sugitani, N. Tamaoki and M. Murayama, “Development of Lattice Welding Robot”, *Technical Commision of Welding Processes, Japan Welding Society*, pp. II–190, 1996

[6] A. Aoki, T. Iizuka, H. Mizuno, S. Yonemoto, and K. Yasuhara, “Multi-purpose Welding System Using Small Portable Robot”, *Welding Guide Book V*, pp. II–214, 2004

[7] D.Y. Lee, J.H. Jung, S.H. Han, Y.J. Lee, and Y.J. Park, “Spider Robot-Automatic Transfer System of the Plasma Welding Machine for LNGC Membrane Sheet”, *ICCAS 2004 Int. Conf. on Control, Automation and Systems*, 2004

[8] J.J Craig, “*Introduction to robotics Mechanics and Control*”, Addison-Wesley, 1989

[9] L.W. Tsai, “*Robot Analysis*”, John Wiley Sons, 1999